Available online at www.sciencedirect.com
SCIENCE DIRECT®
Carbohydrate Research 338 (2003) 69–77
CARBOHYDRATE RESEARCH
www.elsevier.com/locate/carres

# Location of *O*-acetyl substituents in xylo-oligosaccharides obtained from hydrothermally treated *Eucalyptus* wood

Mirjam A. Kabel,[a] Pieter de Waard,[b] Henk A. Schols,[a] Alphons G.J. Voragen[a,*]

[a]*Department of Agrotechnology and Food Sciences, Laboratory of Food Chemistry, Wageningen University, Bomenweg 2, 6703 HD, Wageningen, The Netherlands*

[b]*Wageningen NMR Centre, Laboratory of Biophysics, P.O. Box 8128, 6700 ET, Wageningen, The Netherlands*

Received 10 May 2002; received in revised form 2 September 2002; accepted 23 September 2002

**Abstract**

A combination of techniques was used to localise the *O*-acetyl substituents in xylo-oligosaccharides, which are present in hydrolysates of hydrothermally treated *Eucalyptus* wood. Reversed-phase (RP)-high performance liquid chromatography (HPLC) coupled on-line to both a mass spectrometer and an evaporating light scattering (ELS) detector provided data about the order of elution of the various *O*-acetylated oligomers. The retention of the oligomers on the column depended on the number *and* position of the *O*-acetyl substituents within the xylo-oligosaccharides. One dimensional (1D)- and two dimensional (2D)-$^1$H NMR spectroscopy was used to study the structural features of several xylotetramers separated by RP-HPLC, each having one *O*-acetyl substituent. *O*-Acetyl migration was proven to have occurred in these xylo-oligosaccharides. Mainly *O*-acetyl migration within the same xylosyl residue was observed. RP-HPLC–NMR was performed in order to study the structural features of the acetylated oligomers 'on-line' avoiding *O*-acetyl migration. Finally, the precise location of the 2-*O*- or 3-*O*-acetyl substituent in 6 xylotetramers and 4 xylotrimers separated by RP-HPLC was determined. 

*Keywords:* *O*-Acetyl; Xylo-oligosaccharides; Reversed-phase HPLC; Mass spectrometry; NMR

## 1. Introduction

The wood of *Eucalyptus* is rich in cellulose and hemicellulose, of which the main hemicellulose present is an acetylated 4-*O*-methylglucuronoxylan[1]. Hydrothermal treatment of *Eucalyptus* wood results in a selective fractionation of the hemicellulose and cellulose, which can be used for different product applications.[2,3]

Recently, we described the characterisation of hydrolysates obtained after hydrothermal treatment of *Eucalyptus* wood. More than 60 w/w% of the sugars present in these hydrolysates consists of (*O*-acetyl-)(4-*O*-methylglucurono-) xylo-oligosaccharides.[4,5] Up to now the precise location of the *O*-acetyl substituents within the xylo-oligosaccharides (XOS) present remained unassigned.

The positions of the *O*-acetyl substituents can be studied with the help of linkage analysis.[6–8] However, more rapid and convenient is the use of NMR spectroscopy. York and co-workers have shown that by using a combination of analytical methods, including mass spectrometry (MS) and NMR spectroscopy, the location of the *O*-acetyl substituents on a nonasaccharide repeating unit of xyloglucan can be determined.[9] Several other studies show the presence of *O*-acetyl substituents on xylans or xylan-fragments by directly employing NMR analysis, leaving the exact distribution of the *O*-acetyl substituents over the xylosyl residues out of consideration.[7,10–12]

To be able to assign the precise location of the *O*-acetyl substituents in each of the XOS present in the *Eucalyptus* hydrolysate by using NMR, the oligomers have to be separated first. In the recent literature, the use of reversed-phase (RP) chromatography has been described: e.g., Pauly and co-workers described a method to separate acetylated xyloglucan oligosaccharides by RP chromatography.[13] Other publications de-

* Corresponding author. Tel.: +31-317-482888; fax: +31-317-484893

*E-mail address:* fons.voragen@chem.fdsci.wag-ur.nl (A.G.J. Voragen).

0008-6215/03/$ - see front matter 
PII: S0008-6215(02)00351-8

scribed the use of RP chromatography in for example the separation of a lichenase digest of β-(1-3,(1-4)-D-glucans,[14] maltodextrins[15,16] or even α dextrins with the same degree of polymerisation (DP) but differing in the location of the branch point.[17] An additional advantage of using RP is that the on-line coupling with MS is easy to perform. This has already been reported to be a good tool in the identification of oligosaccharides.[18–20]

In this paper we describe the separation and structural features of several acetylated xylo-oligosaccharides obtained from hydrothermally treated *Eucalyptus* wood by using RP-HPLC–$MS^{(n)}$, NMR and RP-HPLC–NMR.

## 2. Results and discussion

### 2.1. RP-HPLC–MS of acetylated xylo-oligosaccharides

To be able to study the location of the *O*-acetyl substituents in neutral acetylated xylo-oligosaccharides (AcXOS) obtained from hydrothermally treated *Eucalyptus* wood, the AcXOS-mixture was subjected to RP-high performance liquid chromatography (HPLC). The order in which the oligosaccharides present eluted was determined by connecting the RP-column to both an evaporating light scattering (ELS) detector and a mass spectrometer. The ELS-elution pattern and the total ion current (TIC)-elution pattern obtained from the separation of AcXOS by RP-HPLC are presented in Fig. 1. Additionally, the MS-software enabled us to extract 'elution patterns per mass' from the original data (TIC) obtained from the mass spectrometer. Five of such 'elution patterns' are shown in Fig. 2. It was concluded that the number of *O*-acetyl substituents per oligomer influenced their elution by RP-HPLC. The higher the number of *O*-acetyl substituents the longer was the retention of the oligomers on the RP-column used. This resulted in a rather similar retention for oligomers with different DP, but carrying the same number of *O*-acetyl substituents. Similar observations were described by Pauly and co-workers for acetylated xyloglucan oligosaccharides.[13] They showed that the presence of an *O*-acetyl substituent on the galactosyl-residue significantly increased the retention time.

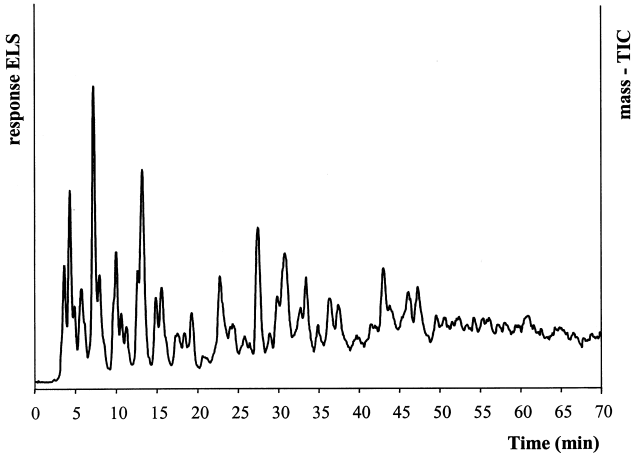


Fig. 1. RP-HPLC elution profiles of AcXOS detected by ELSD and MS (total ion current (TIC)).

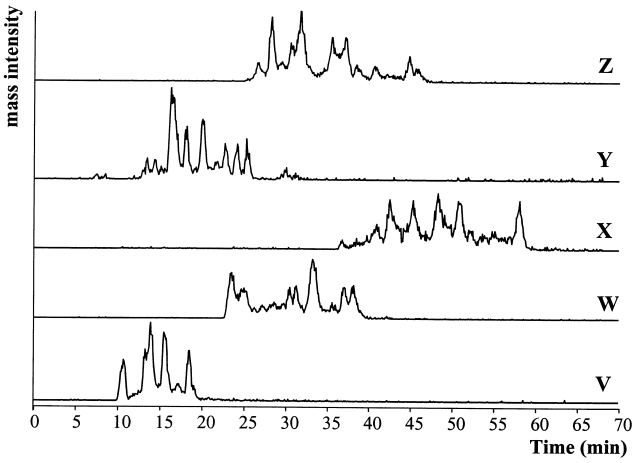


Fig. 2. Elution patterns of mass 479 (V; sodium adducted $X_3Ac$), 521 (W; sodium adducted $X_3Ac_2$), 563 (X; sodium adducted $X_3Ac_3$), 611 (Y; sodium adducted $X_4Ac$) and 653 (Z; sodium adducted $X_4Ac_2$) extracted from the RP-TIC pattern of AcXOS (X = xylose; Ac = *O*-acetyl substituent).

Furthermore, various peaks per mass were eluted (Fig. 2). This can partly be explained by the fact that in general for RP chromatography pairs of peaks are observed corresponding to the α and β anomers of reducing saccharides with a DP ≥ 3.[21] However, separation of α and β anomers alone did not explain the number of peaks eluting per mass.

To determine which of the xylosyl-residues within the various oligomers were acetylated on-line $MS^n$ was performed (not shown). $MS^n$ is reported to be useful in the sequencing of oligosaccharides.[22] However, in the AcXOS studied fragmentation was most likely hindered by the *O*-acetyl substituent(s) present. The higher the number of *O*-acetyl substituents per oligomer the less fragments were observed in the $MS^n$-spectra. Too few fragments were present in the $MS^n$-spectra to be able to determine the location of the *O*-acetyl substituent(s) in the xylo-oligomers.

### 2.2. Location of the *O*-acetyl substituent in a xylotetramer by RP-HPLC–MS

Due to the complexity of the AcXOS-mixture it was decided to study part of the oligomers present in the mixture in more detail. Therefore, the AcXOS-mixture

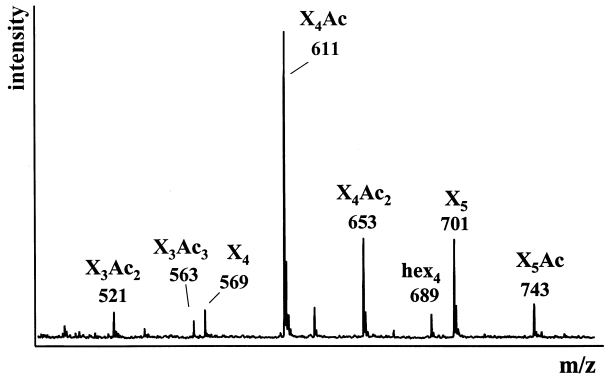


Fig. 3. MALDI-TOF mass spectrum of pool $X_4Ac$; masses are presented as sodium adducts (X = xylose; Ac = *O*-acetyl substituent).

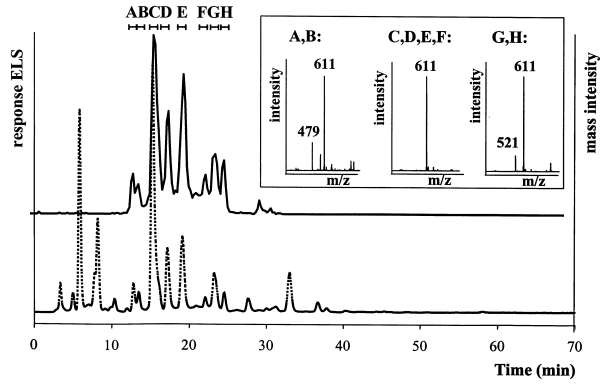


Fig. 4. RP-HPLC elution profiles of AcXOS detected by ELSD (----) and the elution patterns of mass 611 extracted from the RP-TIC pattern (—); the (sum of the) mass spectra of the different peaks encoded by A–H are presented in the inserted window.

was applied to preparative size-exclusion chromatography (BioGel P2).

Fractions obtained from the BioGel P2 column containing mainly mass 611 (sodium adduct of $X_4Ac$) as analysed by MALDI-TOF mass spectrometry were combined and freeze-dried. The MALDI-TOF mass spectrum of the combined pool $X_4Ac$ is presented in Fig. 3. Mainly $X_4Ac$ was accumulated in pool $X_4Ac$, although some other AcXOS were still present as well. Fig. 4 shows the RP-elution pattern of pool $X_4Ac$ detected by ELS. The 'elution pattern' of peaks having mass 611 extracted from the data obtained by the mass spectrometer is presented as well. Mass spectra of peak A–H (Fig. 4) showed that in peak A/B and peak G/H, beside the main $X_4Ac$, only minor signals were detected of mass 479 (sodium adducted $X_3Ac$) and mass 521 ($X_3Ac_2$) respectively. Peaks C, D, E and F solely contained $X_4Ac$. The data obtained from the fragmentation spectra by $MS^n$ of the peaks A–H (not shown) were not conclusive enough to locate the different positions of the *O*-acetyl substituent in the various xylotetramers.

### 2.3. Location of the *O*-acetyl substituent in a xylotetramer by NMR

The pools A, C, D, E, G and H as well as a non-acetylated xylo-oligosaccharide mixture (saponified AcXOS) were subjected to both one-dimensional (1D) and two-dimensional (2D) $^1H$ NMR. The $^1H$ chemical shifts were assigned based on COSY and TOCSY experiments and are presented in Table 1. The $^1H$ NMR resonances of non-acetylated xylo-oligosaccharides were used as a reference for reducing end xylose residues ($X_{red\ \alpha}$ and $X_{red\ \beta}$), internal ($X_i$) and non-reducing end ($X_t$) xylosyl residues. These $^1H$ chemical shifts (Table 1) were in good agreement with values published earlier.[1,23–25]

The NMR spectra obtained from pool C were similar to the ones of pool E and H. In these spectra particular signals were obtained for a reducing end xylose residue (α and β), of which the H-1 was shifted slightly upfield (($X_i2$-)$\mathbf{X_{red\alpha/\beta}}$). An internal xylosyl residue, of which the H-1 was shifted upfield was observed ($\mathbf{X_i}$(-$X_i3$)) and a non-reducing end residue ($X_t$), and both an internal 2-*O*- and 3-*O*-acetylated xylosyl residue ($X_i2$ and $X_i3$) could be distinguished. Therefore, we assumed that the pools C, E and H represented a mixture of xylotetramers (α and β) with the 2-*O*- or 3-*O*-acetyl substituent located on the second xylosyl residue from the reducing end. This assumption was strengthened by the results presented by Van Hazendonk and co-workers.[12] They showed that the H-1 of a non-acetylated internal xylosyl residue linked to an 3-*O*-acetylated xylose was shifted upfield.

The spectra of pool D were similar to pool G. A particular signal ($\mathbf{X_t}$(-$X_i3$)) was observed in these spectra of a non-reducing end xylosyl of which the H-1 was shifted slightly upfield compared to a $X_t$-residue. This upfield-shift was comparable with the upfield-shift observed in the pools C, E and H between the H-1 of the $\mathbf{X_i}$(-$X_i3$) and $X_i3$-residue. A $X_{red\ \alpha}$- and $X_{red\ \beta}$-, $X_i3$- and $X_i2$-residue were distinguished as well. Combining these results, it was assumed that the pools D and G contained a mixture of xylotetramers (α and β) with the 2-*O*- or 3-*O*-acetyl substituent located on the third residue (counting from the reducing end residue).

In the spectra of pool A signals were observed corresponding to 2-*O*- and 3-*O*-acetylated xylosyl residues with $^1H$ chemical shifts shifted upfield compared to a $X_i2$- and $X_i3$-residue. These upfield-shifts corresponded well with the upfield-shifts observed between an $X_i$- and $X_t$-residue. A $X_{red\ \alpha}$- and $X_{red\ \beta}$-residue and a $X_i$-residue were distinguished as well. Therefore, we assumed that pool A represented a mixture of xylotetramers (α and β) with the 2-*O*- or 3-*O*-acetyl substituent located on the non-reducing end xylosyl residue. To our knowledge this is the first time that $^1H$ chemical shifts for acetylated non-reducing end xylosyl residues are presented ($X_t2$ and $X_t3$; Table 1).

The $^1$H chemical shifts observed in the different pools for both the internal 2-*O*-acetylated and internal 3-*O*-acetylated xylosyl residues ($X_i2$ and $X_i3$; Table 1) corresponded well with values reported in literature.[10,12] The $^1$H chemical shifts of xylosyl residues neighbouring $X_i2$- or $X_i3$-residues were partly described in literature.[10,12] However, the assignment of the signals to the corresponding xylosyl residues was not performed yet. In the current study we were able to assign the $^1$H chemical shifts to the corresponding xylosyl residue next to a $X_i2$- or $X_i3$-residue as discussed in the previous part of the text (($X_i2$-)$\mathbf{X_{red\alpha/\beta}}$, $\mathbf{X_i}$(-$X_i3$), $\mathbf{X_t}$(-$X_i3$); Table 1). The assignment was completed only in combination with the results obtained by RP-HPLC–NMR (Section 2.4).

Some deacetylation was apparent from the presence of signals corresponding to non-acetylated xylose and xylosyl residues in each position ($X_{red\alpha/\beta}$-, $X_i$- and $X_t$-residue) in all pools analysed each of the pools contained a mixture of 2-*O*- and 3-*O*-acetylated xylotetramers with the *O*-acetyl substituent at the same xylosyl residue per pool. Therefore, the pools were resubjected to RP-HPLC–MS (Fig. 5) and it was shown that more peaks having mass $X_4$Ac eluted (12–26 min) than the expected two peaks (α and β) per pool.[21] All oligomers eluting between 12 and 26 min from the RP-column were $X_4$Ac-oligomers, which was confirmed by RP-HPLC–MS ($m/z$ 611 (sodium-adduct); not shown). The same peaks were eluted for pool C and E with similar intensities. The same observations were made for pools D and G. The most reasonable explanation for these results was that *O*-acetyl migration had occurred within the xylotetramer after pooling from RP-HPLC. Unambiguous evidence for this assumption is presented in Section 2.5. Additionally, resubmitting of the pools revealed that besides *O*-acetyl migration indeed deacetylation had occurred as expected from the NMR-results. Both α and β xylotetraose were distinguished with a retention time of about 8.5 and 6 min respectively in the ELS (Fig. 5) and RP-HPLC–MS chromatograms ($m/z$ 569 (sodium-adduct); not shown).

### 2.4. Location of the *O*-acetyl substituent in a xylotetramer by LC–NMR

We aimed to use RP-HPLC–NMR on-line, since already a mild sample handling starting from collection of fractions till NMR-measurements (evaporation of

Table 1
Summary of $^1$H chemical shifts (ppm) of the various xylose and xylosyl residues observed in COSY and TOCSY spectra of pool A, C, D, E, G and H

| Pool | Structure [a] | Xylose residue [b] | $^1$H chemical shifts in ppm | | | | | |
|---|---|---|---|---|---|---|---|---|
| | | | H-1 | H-2 | H-3 | H-4 | H-5ax | H-5eq |
| A; C = E = H; D = G | I, I*, II, III, IV, VII | $\mathbf{X_{red\ \alpha}}$ | 5.18 | 3.55 | 3.83 | 3.76 | 3.98 | 3.76 |
| A; C = E = H; D = G | I, I*, II, III, IV, VII | $\mathbf{X_{red\ \beta}}$ | 4.58 | 3.24 | 3.55 | 3.78 | 3.38 | 4.05 |
| A; C = E = H; D = G | I, I*, III, IV, V, VII | $\mathbf{X_i}$ | 4.48 | 3.28 | 3.56 | 3.79 | 3.40 | 4.10 |
| A; C = E = H; D = G | II, III, V | $\mathbf{X_t}$ | 4.46 | 3.26 | 3.43 | 3.63 | 3.32 | 3.97 |
| C = E = H; D = G | I, II, IV, VII | $\mathbf{X_i3}$ | 4.58 | 3.48 | 4.99 | 3.94 | 3.48 | 4.12 |
| C = E = H; D = G | I*, III, V | $\mathbf{X_i2}$ | 4.71 | 4.71 | 3.79 | 3.86 | 3.45 | 4.15 |
| C = E = H | V | ($X_i2$-)$\mathbf{X_{red\ \alpha}}$ | 5.17 | nd [c] | nd [c] | nd [c] | nd [c] | nd [c] |
| C = E = H | V | ($X_i2$-)$\mathbf{X_{red\ \beta}}$ | 4.55 | 3.24 | nd [c] | nd [c] | nd [c] | nd [c] |
| C = E = H | II | $\mathbf{X_i}$(-$X_i3$) | 4.44 | 3.21 | 3.53 | 3.74 | 3.38 | 4.04 |
| D = G | IV, VII | $\mathbf{X_t}$(-$X_i3$) | 4.42 | 3.17 | 3.42 | 3.6 | 3.32 | 3.94 |
| A | I | $\mathbf{X_t3}$ | 4.57 | 3.45 | 4.9 | 3.81 | 3.45 | 4.02 |
| A | I* | $\mathbf{X_t2}$ | 4.68 | 4.68 | 3.65 | 3.72 | 3.35 | 4.03 |

[a] Structure I–VII as indicated in Fig. 7.

[b] $\mathbf{X_{red\ \alpha/\beta}}$, reducing end Xyl; $\mathbf{X_i}$, internal Xyl; $\mathbf{X_t}$, non-reducing end Xyl; $\mathbf{X_i3}$, 3-*O*-acetylated internal Xyl; $\mathbf{X_i2}$, 2-*O*-acetylated internal Xyl; ($X_i2$-)$\mathbf{X_{red\ \alpha/\beta}}$, reducing end Xyl substituted (4→1) with $X_i2$; $\mathbf{X_i}$(-$X_i3$), internal Xyl linked (1→4) with $X_i3$; $\mathbf{X_t}$(-$X_i3$), non-reducing end Xyl linked (1→4) with $X_i3$; $\mathbf{X_t3}$, 3-*O*-acetylated non-reducing end Xyl; $\mathbf{X_t2}$, 2-*O*-acetylated non-reducing end Xyl.

[c] Not detected.

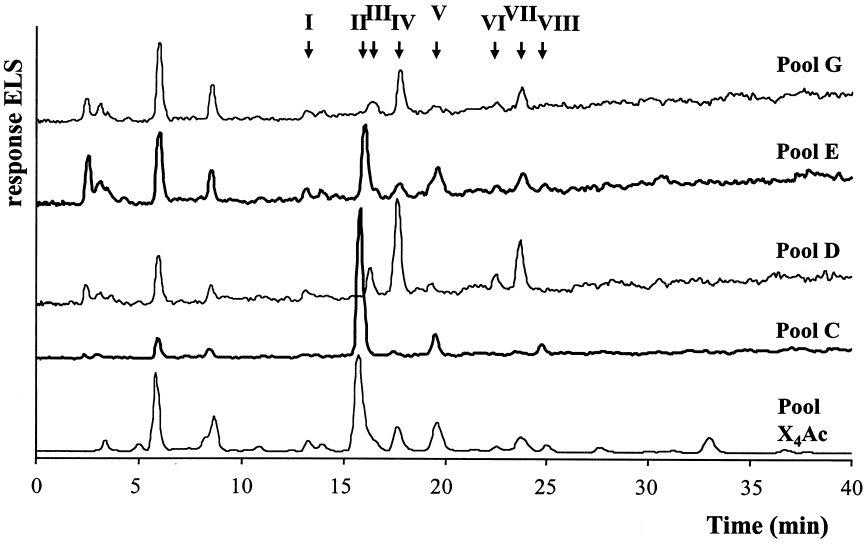


Fig. 5. RP-HPLC elution profiles of pool $X_4Ac$, C, D, E, and G detected by ELSD; peaks containing a xylotetramer with one *O*-acetyl substituent are encoded I–VIII.

methanol, freeze-drying and freeze-drying in $D_2O$) most likely promoted *O*-acetyl migration (Section 2.3). Furthermore, for further research it is important to know which RP-peak (Fig. 4) belonged to which structure revealed by NMR as presented in Section 2.3.

Pool $X_4Ac$ and the pools C and D (Fig. 4) were applied to RP-HPLC–NMR (Fig. 6). The numbers II–V and VII in Fig. 6 correspond with the peaks II–V and VI in Fig. 5, representing the different xylotetramers with one *O*-acetyl substituent. The peaks I, VI and VIII were too low in concentration in all samples applied to RP-HPLC–NMR to obtain good signals for the NMR-spectra. The peaks coded I–VIII represented similar oligomers as the originally pooled oligomers coded A–H (Fig. 4). Therefore, results obtained by the RP-HPLC–NMR performed could be compared well with the NMR-results described in Section 2.3.

Oligomers II, IV, V and VII eluted by RP solely contained one $X_4Ac$, also indicated by only one $^1H$ chemical shift observed for the $CH_3$ group of the *O*-acetyl substituent present (2.15 or 2.16 ppm).[10,12] The 1D-spectra corresponding to oligomer III showed two *O*-acetylated oligomers (Fig. 6). However, together with oligomer III some material of oligomer II was coeluted (Fig. 5). The signal detected around 2.05 ppm resulted from an impurity of acetonitrile. The position of the *O*-acetyl substituent (2-*O* or 3-*O*) was rather easy to determine from the 1D-spectra obtained. Namely, the H-2 and H-3 of the 2-*O*- and 3-*O*-acetylated xylosyl residue respectively gave well distinguishable signals in the anomeric region of the 1D-spectra (see Section 2.3 as well). The anomeric signals of the $X_{red\ \alpha/\beta}$-, $X_i$- and $X_t$-residue shown in Fig. 6 were rather easy to assign as well, since for each pure xylotetramer only four different anomeric protons (residues) could be

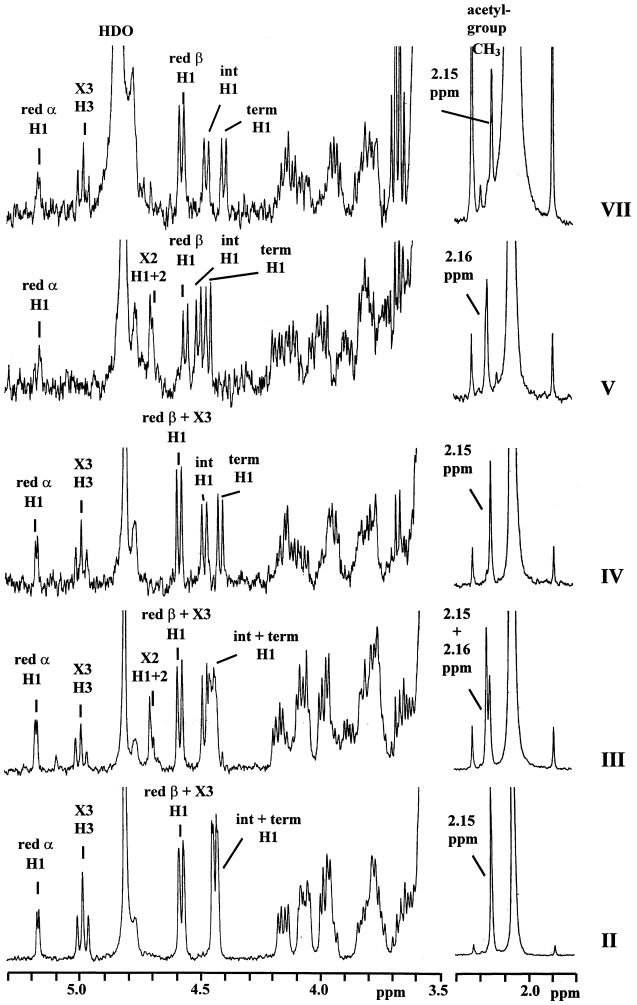


Fig. 6. 1D $^1H$ NMR spectra obtained by RP-HPLC–NMR of peak II–V and VII.

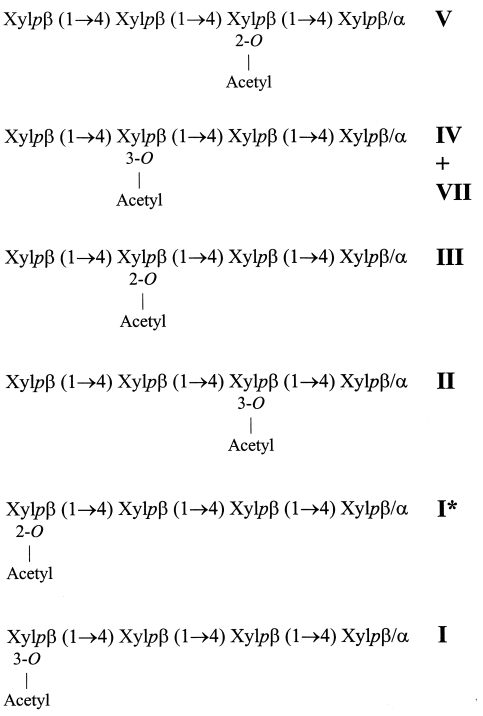


Fig. 7. Summary of structures of the various xylotetramers with one *O*-acetyl substituent, eluting in the RP-peaks I–V and VII. Peak I and I* were present in pool A (Section 2.3).

present per 1D-spectrum. Additionally, part of the signals had already been assigned as described in Section 2.3.

Combining the 1D-results of the purely obtained acetylated xylotetramers (Fig. 6) with the TOCSY-results of the pools A–H (Section 2.3), a complete assignment of the $^1$H-shift of the different xylosyl residues was obtained (Table 1). The structures resulting from this Table of the xylotetramers including the location of the *O*-acetyl substituent are presented in Fig. 7.

A disadvantage of storing the RP-peaks in the BPSU before NMR analysis is the re-establishment of the α/β equilibrium. Therefore, a distinction between the α and β anomeric form separated by RP-HPLC was not obtained by the NMR performed. The amounts of sample were too low for direct RP-HPLC–NMR measurements.

## 2.5. Migration of the *O*-acetyl substituent in a xylotetramer

The different structures of the acetylated xylotetramers corresponding to the RP-peaks (Fig. 7) demonstrated that *O*-acetyl migration had occurred within the pools A–H as had already been suggested in Section 2.3. In pool C and D, which originally contained structure II and IV respectively (Fig. 7 and Section 2.4), part of the 3-*O*-acetyl substituents were migrated to the 2-*O*-position of the same xylosyl residue resulting in structure V and III respectively (Figs. 5 and 7). Similarly, in pool E, which originally contained structure V (Fig. 7 and Section 2.4), part of the 2-*O*-acetyl substituents were migrated to the 3-*O*-position of the same xylosyl residue resulting in structure II (Figs. 5 and 7). The same equilibrium was reached starting from either the 2-*O*- or the corresponding 3-*O*-acetylated tetramer, in favour of the 3-*O*-acetylated compounds. *O*-Acetyl migration was only observed within the same xylosyl residue.

To our knowledge, this is the first time that *O*-acetyl migration was proven in xylo-oligosaccharides in such detail. Reicher and co-workers and Biely and co-workers have already observed that *O*-acetyl migration took place in aqueous solutions of methyl 2-*O*-acetyl-4-*O*-methyl-β-D-xylopyranoside.[26,27] Reicher and co-workers did not observe any *O*-acetyl migration in xylan from hardwood (*Mimosa scabrella*) during treatment with aqueous chlorine or hot ethanol.[26] However, it is possible that the ratio of 2-*O*- and 3-*O*-acetyl substituents in the xylan is close to that of an equilibrium mixture,[6] so that any *O*-acetyl migration could not be detected. *O*-Acetyl migration is observed as well within the compounds benzyl 2-*O*-acetyl-4-*O*-methyl-β-D-xylopyranoside and benzyl 3-*O*-acetyl-4-*O*-methyl-β-D-xylopyranoside affected by various chemicals.[28] Finally, *O*-acetyl migration is reported to occur in acetylated inositol derivatives and xyloglucan oligosaccharides.[13,29]

Some minor experiments were carried out to study the conditions under which *O*-acetyl migration occurred. Material present in separate loops in the BPSU of the LC–NMR apparatus each containing pure acetylated tetramers in ($D_2O$/methanol) were kept for about 1 h at 70 °C or for about 3 days at 20 °C. At these conditions no *O*-acetyl migration was observed. So, it is still questionable why the freezedrying and/or re-dissolving the material in $D_2O$ performed already had promoted the *O*-acetyl migration as described in Sections 2.3 and 2.4.

Taking in account these observations, it was expected that *O*-acetyl migration and deacetylation might have occurred during hydrothermal treatment of the *Eucalyptus* wood as well. Therefore, the position and distribution of the *O*-acetyl substituents in the xylo-oligomers analysed can not be extrapolated directly to the xylan-structures originally present.

## 2.6. Location of the *O*-acetyl substituent in a xylotrimer by LC–NMR

To present the possibilities of RP-HPLC–NMR confirming the location of *O*-acetyl groups in other xylo-oligosaccharides than xylotetramers, a sample containing mainly *O*-acetylated xylotrimers was analysed.

The *O*-acetyl substituent in xylotrimers present in the AcXOS-mixture (Section 2.1) could be located similarly to the determination of the location of the *O*-acetyl substituent in a xylotetramer. The AcXOS-mixture had already been fractionated by size-exclusion chromatography and also fractions in which mainly a $X_3Ac$ was present were obtained. Four of these fractions were combined to pool $X_3Ac$ and this pool was subjected to RP-HPLC–NMR. The RP-chromatogram resembled the elution pattern as presented in Fig. 2(V).

A TOCSY-spectrum was obtained of the material represented by the highest peak in the RP-chromatogram (Fig. 8). The signals obtained (Fig. 8) were comparable with the $^1$H-shifts summarised in Table 1, which resulted in the characterisation of the two structures presented in Fig. 8. Furthermore, this TOCSY-spectrum was of help in identifying the 1D-NMR spectra obtained of several other acetylated xylotrimers separated by RP-HPLC–NMR. These represented mainly xylotrimers with the 2-*O*- or 3-*O*-acetyl substituent located to the non-reducing end xylosyl residue.

### 2.7. Concluding remarks

*O*-acetyl substituted xylo-oligosaccharides were separated by using RP-HPLC. An advantage of using RP-HPLC was that only pure water and methanol were used for the separations, facilitating the on-line coupling to a mass spectrometer. High pH high performance anion-exchange chromatography (HPAEC) using salt gradient up to 1 M, which also is a commonly used technique to separate oligosaccharides,[30,31] is more difficult to perform on-line with a mass spectrometer. Although, a successful off-line combination of HPAEC with MALDI-TOF MS has been described.[32] However, at the high pH used in HPAEC *O*-acetyl substituents will be removed and was no option to use. By using RP-HPLC–MS it became possible

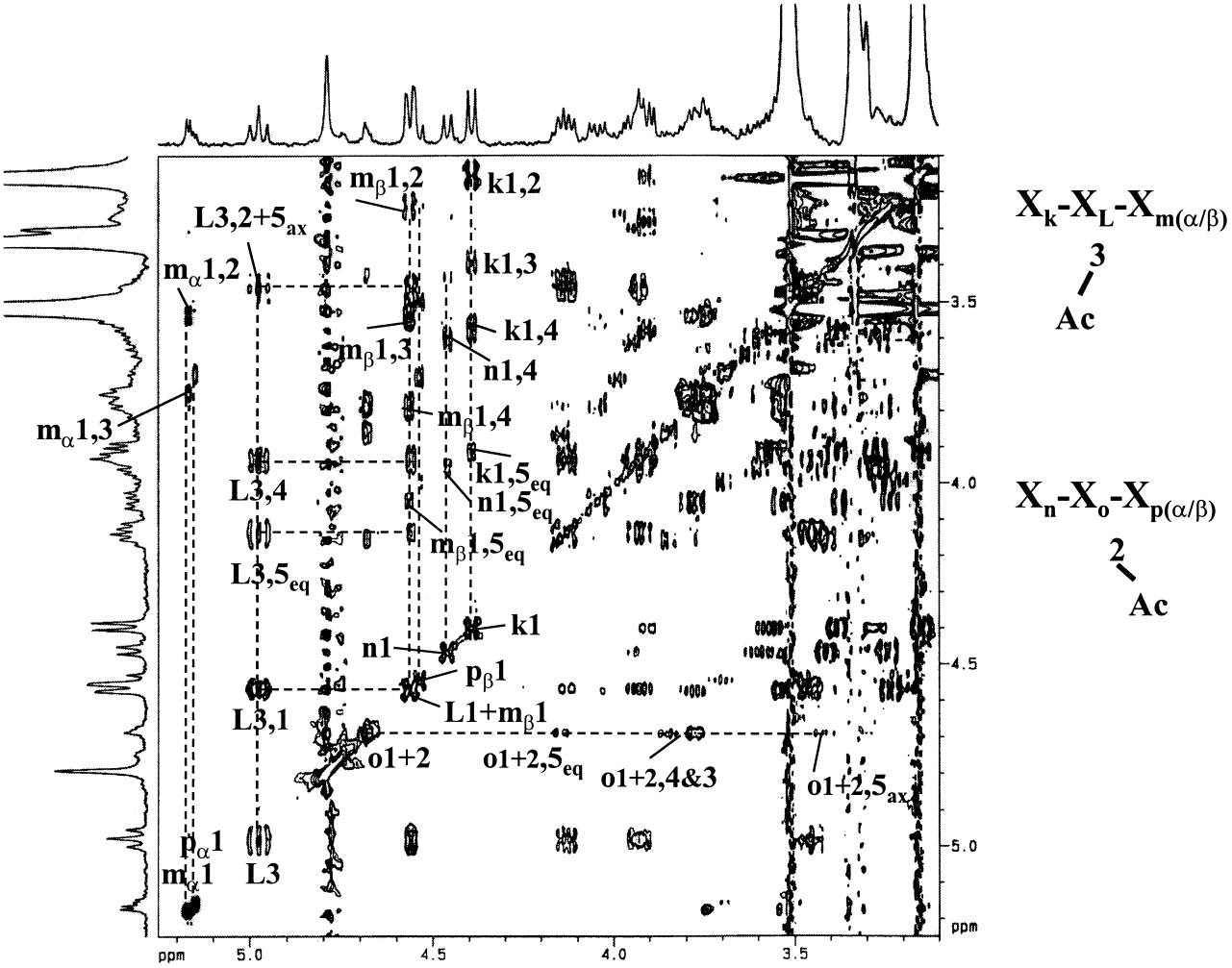


Fig. 8. 2D TOCSY spectrum of pool $X_3Ac$. Diagonal peaks and corresponding cross-peaks of the anomeric protons of the various residues (encoded K–P) present are indicated. The two structures deduced from this spectrum are presented as well.

to separate and detect xylo-oligomers having the same DP, but in which the *O*-acetyl substituent was located at different positions.

To identify the precise location of the *O*-acetyl substituent in both xylotetramers and xylotrimers RP-HPLC–NMR combined with an intermediate BPSU was used. 1D-NMR spectra were obtained of most of the oligomers by the RP-HPLC–NMR performed. Concentrations used were 50–150 μg per peak for determining 1D-NMR spectra in 2–4 h and at least 150 μg per peak to obtain a TOCSY-spectrum about 50 h.

In conclusion, by RP-HPLC–MS, NMR and RP-HPLC–NMR we were able to localise the *O*-acetyl substituent in 6 xylotetramers and 4 xylotrimers. Additionally, to our knowledge for the first time *O*-acetyl migration was proven to have occurred in xylo-oligosaccharides.

## 3. Experimental

### 3.1. Acetylated xylo-oligosaccharides

The neutral acetylated XOS (AcXOS) were obtained as described previously.[5]

### 3.2. Size-exclusion chromatography

To fractionate the AcXOS-mixture (163 mg in 2 mL) a Pharmacia system equipped with a BioGel P-2 column (900 × 26 mm; 200–400 mesh, Bio-Rad Laboratories) thermostated at 60 °C was used. Elution was performed at 0.5 mL/min with water (60 °C) and fractions were collected every 2 mL. The eluent was detected by a Shodex RI-72 detector. Four of these size-exclusion runs were performed to obtain sufficient material of pool $X_4Ac$.

### 3.3. MALDI-TOF mass spectrometry

Matrix assisted laser desorption/ionisation time-of-flight mass spectrometry (MALDI-TOF MS) was performed as described before.[5]

### 3.4. Reversed-phase HPLC–mass spectrometry

Reversed-phase HPLC was performed on a HPLC system (Thermo Separation Products) equipped with a Thermohypersil Aquasil C18 column ((Keystone Scientific); 4.6 mm ID × 150 mm; 3 μm) in combination with a Thermohypersil Aquasil C18 guard column (4.6 mm ID × 10 mm; 3 μm). The RP-column was coupled to a splitter (Dionex) directing 10% of the eluent to a Sedex 55 evaporating light scattering detector (Sedere), 5% to a LCQ Ion-trap (Finnigan MAT 95) and the remaining part to a fraction collector or waste. Elution (0.8 mL/min) was performed using a gradient of degassed (Membrane degasser; Thermo Separation Products) methanol in pure water: 0–28 v/v% methanol in 0–70 min. Each elution was followed by a equilibration step (isocratic pure water; 30 min). Pool $X_4Ac$ (20 mg/mL) was subjected to RP chromatography separated in 20 RP-HPLC runs (20 times 100 μL of injection) to obtain enough material of each peak to perform NMR analysis. Fractions (276 μL) were collected by using a fraction collector in the same series of tubes for 5 runs. Finally, all tubes containing similar material were combined.

MS analysis was carried out in the positive mode using a spray voltage of 5.5 kV and a capillary temperature of 200 °C. The capillary voltage was set at 42 kV and the tube lens voltage at 20 kV. $MS^n$ was performed using a window of 1.5–2 $m/z$ and a 35–40% relative collision energy. The apparatus and the data were controlled by Xcalibur software. The accuracy of the mass determinations is $\pm 0.3$ Da.

### 3.5. NMR spectroscopy

Samples were exchanged in $D_2O$ (99.9 atom% D, Cambridge Isotope Laboratories) with intermediate freeze drying, dissolved in 190 μL 99.96% $D_2O$ (Cambridge Isotope Laboratories) and inserted in NMR Shigemi-microtubes. NMR spectra were recorded at a probe temperature of 25 °C on a Bruker AMX-500 spectrometer located at the Wageningen NMR Centre. $^1H$ chemical shifts are expressed in ppm relative to internal acetone ($\delta$ 2.225). 1D $^1H$ NMR spectra were recorded at 500.13 MHz using 64 scans of 8192 data points and a sweep width of 3000 Hz. The 2D COSY spectra were acquired using the double quantum filtered (DQF) method with a standard pulse sequence delivered by Bruker. The 2D TOCSY spectra were acquired using standard Bruker pulse sequences with a mixing time of 100 ms. For these 2D $^1H$ spectra 512 experiments of 2048 data points were recorded using 32 scans per increment.

### 3.6. Reversed-phase HPLC–NMR

Reversed-phase HPLC–NMR was performed on a HPLC system (Bruker) equipped with a Thermohypersil Aquasil C18 column (4.6 mm ID × 150 mm; 3 μm) in combination with a Thermohypersil (Keystone Scientific) Aquasil C18 guard column (4.6 mm ID × 10 mm; 3 μm). Furthermore, the HPLC system was connected to a Bruker peak sampling unit (BPSU; Bruker) following UV detection (205–215 nm; Bruker). Elution (0.8 mL/min) was performed using a gradient of degassed (Membrane degasser; Bruker) methanol in $D_2O$: 0–16 v/v% methanol in 0–40 min. Samples containing mainly $X_4Ac$ ($\sim$10 mg/mL) or $X_3Ac$ ($\sim$15 mg/mL),

obtained by size-exclusion chromatography, were applied to RP-HPLC–NMR (100 μL/run). Each elution was followed by a equilibration step (isocratic $D_2O$; 30 min). Samples were transported one by one from the BPSU to the NMR probe, using the same ratio of $D_2O$/methanol as was necessary for the particular oligomers to elute from the RP-column.

NMR spectra were recorded at a probe temperature of 25 °C on a Bruker DPX-400 spectrometer located at the Wageningen NMR Centre. Solvent signals were suppressed with double presaturation using Bruker LC–NMR software. $^1$H chemical shifts are expressed in ppm relative to methanol ($\delta$ 3.34). 1D $^1$H NMR spectra were recorded at 400 MHz using up to 2000 scans of 32,768 data points and a sweep width of 8000 Hz. The 2D TOCSY spectrum was acquired using a standard Bruker pulse sequence. 496 experiments of 2048 data points were recorded using 240 scans per increment resulting in a measuring time of 66 h. The mixing time was 65 ms.

## 4. Supplementary material

The material is available from the authors on request.

## Acknowledgements

The authors are grateful to the EU for their financial support (FAIR CT98-3811). We thank Ing.R.V. for performing part of the NMR-analysis.

## References

1. Shatalov, A. A.; Evtuguin, D. V.; Neto, C. P. *Carbohydr. Res.* **1999**, *320*, 93–99.
2. Garrote, G.; Dominguez, H.; Parajó, J. C. *J. Chem. Technol. Biotechnol.* **1999**, *74*, 1101–1109.
3. Koukios, E. G.; Pastou, A.; Koullas, D. P.; Sereti, V.; Kolosis, F. New green products from cellulosics. In *Biomass*: *A Growth Opportunity in Green Energy and Value-added Products*; Overend, R. P.; Chornet, E., Eds.; Permagon: Oxford, 1999; p 641.
4. Kabel, M. A.; Carvalheiro, F.; Garrote, G.; Avgerinos, E.; Koukios, E.; Parajó, J. C.; Gírio, F. M.; Schols, H. A.; Voragen, A. G. J. *Carbohydr. Polym.* **2002**, *50*, 47–56.
5. Kabel, M. A.; Schols, H. A.; Voragen, A. G. J. *Carbohydr. Polym.* **2002**, *50*, 191–200.
6. Lindberg, B.; Rosell, K.-G.; Svensson, G. *Svensk Papperstidning* **1973**, *76*, 30–32.
7. Karacsonyi, S.; Alfoldi, J.; Kubackova, M.; Stupka, L. *Cellul. Chem. Technol.* **1983**, *17*, 637–645.
8. Reicher, F.; Correa, J. B. C. *Carbohydr. Res.* **1984**, *135*, 129–140.
9. York, W. S.; Oates, J. E.; Van Halbeek, H.; Darvill, A. G.; Albersheim, P. *Carbohydr. Res.* **1988**, *173*, 113–132.
10. Teleman, A.; Lundqvist, J.; Tjerneld, F.; Stalbrand, H.; Dahlman, O. *Carbohydr. Res.* **2000**, *329*, 807–815.
11. Korte, H. E.; Offermann, W.; Puls, J. *Holzforschung* **1991**, *45*, 419–425.
12. Van Hazendonk, J. M.; Reinerink, E. J. M.; De Waard, P.; Van Dam, J. E. G. *Carbohydr. Res.* **1996**, *291*, 141–154.
13. Pauly, M.; York, W. S. *Am. Biotech. Lab.* **1998**, 14.
14. Perez-Vendrell, A. M.; Guasch, J.; Francesch, M.; Molina cano, J. L.; Brufau, J. *J. Chromatogr., Sect. A* **1995**, *718*, 291–297.
15. Cheetham, N. W. H.; Sirimanne, P. *J. Chromatogr.* **1981**, *207*, 439–444.
16. Ciesarova, Z.; Smogrovicova, D.; Sajbibor, J.; Magdolen, P. *Biotechnol. Tech.* **1995**, *9*, 869–872.
17. Jodelet, A.; Rigby, N. M.; Colquhoun, I. J. *Carbohydr. Res.* **1998**, *312*, 139–151.
18. Hulthe, G.; Stenhagen, G.; Fogelquist, E. *J. Chromatogr., Sect. A* **1997**, *777*, 141–153.
19. Niessen, W. M. A. *J. Chromatogr., Sect. A* **1999**, *856*, 179–197.
20. Niessen, W. M. A.; Van der Hoeven, R. A. M.; Van der Greef, J.; Schols, H. A.; Voragen, A. G. J. *Rapid Commun. Mass Spectrom.* **1992**, *6*, 197–202.
21. Rassi, Z. E. *J. Chromatogr., Sect. A* **1996**, *720*, 93–118.
22. Brull, L. P.; Huisman, M. M. H.; Schols, H. A.; Voragen, A. G. J.; Critchley, G. *J. Mass Spectrom.* **1998**, *33*, 713–720.
23. Hoffmann, R. A.; Leeflang, B. R.; De Barse, M. M. J.; Kamerling, J. P.; Vliegenthart, J. F. G. *Carbohydr. Res.* **1991**, *221*, 63–81.
24. Gruppen, H.; Hoffmann, R. A.; Kormelink, F. J. M.; Voragen, A. G. J.; Kamerling, J. P.; Vliegenthart, J. F. G. *Carbohydr. Res.* **1992**, *233*, 45–64.
25. Broberg, A.; Thomsen, K. K.; Duus, J. O. *Carbohydr. Res.* **2000**, *328*, 375–382.
26. Reicher, F.; Gorin, F. A. J.; Sierakowski, M.-R.; Correa, J. B. C. *Carbohydr. Res.* **1989**, *193*, 23–31.
27. Biely, P.; Cote, G. L.; Kremnicky, L.; Weisleder, D.; Greene, R. V. *Biochim. Biophys. Acta* **1996**, *1298*, 209–222.
28. Garegg, J. *Acta Chem. Scand.* **1962**, *16*, 1849–1857.
29. Angyal, S. J.; Melrose, G. J. H. *J. Chem. Soc.* **1965**, 6494–6500.
30. Lee, Y. C. *Anal. Biochem.* **1990**, *189*, 151–162.
31. Lee, Y. C. *J. Chromatogr., Sect. A* **1996**, *720*, 137–149.
32. Kabel, M. A.; Schols, H. A.; Voragen, A. G. J. *Carbohydr. Polym.* **2001**, *44*, 161–165.